We are IntechOpen,
the world's leading publisher of Open Access books
Built by scientists, for scientists

6,900
Open access books available

185,000
International authors and editors

200M
Downloads

154
Countries delivered to

Our authors are among the

TOP 1%
most cited scientists

12.2%
Contributors from top 500 universities

CLARIVATE ANALYTICS
BOOK CITATION INDEX
INDEXED

WEB OF SCIENCE™

Selection of our books indexed in the Book Citation Index
in Web of Science™ Core Collection (BKCI)

Interested in publishing with us?
Contact book.department@intechopen.com

Numbers displayed above are based on latest data collected.
For more information visit www.intechopen.com

Myoblast Differentiation of Umbilical Cord Blood Derived Stem Cells on Biocompatible Composites Scaffold Meshes

Biswadeep Chaudhuri

Abstract

Tissue Engineering (TE) is emerging as an effective way of curing different tissue oriented disorders and new tissue regeneration. Here, it has been attempted to show that biocompatible graphene oxide nanoplatelets (GOnPs)-polymer nanocomposites are novel materials for the fabrication of TE scaffolds for myoblast differentiation of human umbilical cord blood derived mesenchymal stem cells (CB-hMSCs). Addition of GOnPs in bioactive polymers like PCL (poly-caprolactone) and GO-PLGA (poly lactic co-glycolic acid) enhances electrical conductivity and biocompatibility of the electro-spun composite scaffolds. CB-hMSCs were used for the direct differentiation to skeletal muscle cells (hSkMCs) on the electrospun GOnPs–PCL and GOnPs-PLGA nanocomposite scaffolds. These scaffolds exhibited admirable myoblast differentiation, proliferation and also promoted self-aligned myotubes formation. Moreover, IGF-1 cell signaling pathway study carried out on GOnPs-PCL composite scaffold meshes also showed their potentiality for excellent myoblast differentiation and proliferation. Structural, mechanical, microstructural and vibration spectroscopic studies were carried out to characterize the scaffold materials. Significantly enhanced values of both conductivity and dielectric constant provided favorable cues for the increase of cells-scaffold interaction and biocompatibility of GOnPs based polymer composite scaffolds. Present study confirmed GOnPs-polymer composite scaffolds as the potential candidates for the myoblast differentiation of CB-hMSCs for skeletal muscle or other tissues repair and regenerations.

Keywords: umbilical cord blood, mesenchymal stem cells, myoblast differentiation, graphene oxide, polymer nanocomposite, electrospinning

1. Introduction

Fabricated artificial scaffolds using suitable biomimetic substrates were found to control the cellular behaviour and deliver appropriate cues for the differentiation and proliferation of different cell types for tissue engineering (TE) applications. Ideal scaffolds directly or indirectly help the growth of cells because they interact with the cells. Excellent biocompatibility, antibacterial property and mechanical stability of the scaffolds are necessary to provide adequate environment for cell growth and proliferation. Over the last decade, various nanomaterials (nanodiamond, graphene and carbon nanotubes) have been used along with suitable polymer to meet the requirements of the desired scaffold materials [1].Among the various techniques used for the fabrications of scaffolds, electrospinning drew worldwide attention as a simple and effective method [2] of preparing scaffold meshes of different biocompatible polymers like poly-caprolactone (PCL), polyvinyl alcohol (PVA) and poly(lactic-co-glycolic acid (PLGA)). These polymers have extensively been used for TE and biomedical applications [3–5] because of their appropriate biocompatibility, biodegradability and good solubility in different organic solvents. However, as the values of both conductivity ($\sigma \sim 10^{-9}$ S/m) and dielectric permittivity ($\varepsilon < 10$) of most of these bioactive polymers are extremely small and also highly biodegradable; these polymers alone are not very suitable for many electronic as well as biomedical applications. Conducting polymers like polyaniline (PANi) and other solid materials blended with insulating polymers (such as PCL and PLGA PVA) were found to enhance biocompatibility, biodegradability and better cell scaffolds constructs [5, 6]. Interestingly, addition of very small amount (~0.3–0.5 wt%) of graphene oxide (GO) nanoplatelets (GOnPs) in different polymers like poly(methyl methacrylate) (PMMA) [7] and polyvinyl alcohol (PVA) [8] were reported to enhance both ε and σ values of the resulting composites by 2–3 orders of magnitudes along with enhancement of thermomechanical stability [8]. Conductivity enhancement of the scaffolds was also reported to provide important cues for myoblast differentiation [9].

Graphene oxide (GO) or reduced graphene oxide (rGO) are the oxidized forms of graphene. These oxides possess many oxygen-containing functional groups, such as hydroxyl, carboxyl and epoxy groups, and they can also adsorb small molecular weight chemical [10] which favour cell-scaffold interaction and cell viability. Therefore, graphene oxides might be considered as suitable biocompatible filler materials for making polymer composites for different biomedical and clinical applications. Moreover, chemically synthesized GO and rGO have also attracted more interest instead of graphene, in some respects, due to their extraordinary physicochemical properties, ease of synthesis in pure form and fabrication for applications in drug delivery [11], cancer therapies [12] and TE [13, 14].

Other than scaffolds, another important issue of tissue engineering is the availability of constant supply of stem cells which are mostly procured from bone marrow (BM), adipose tissue, etc. It is rather difficult to obtain these stem cells requiring sophisticated surgical procedures. Moreover, there are also problems to find appropriate donors. However, it has already been established that human umbilical cord blood, considered to be a biological waste,

is an import and cost effective source of mesenchymal stem cells (MSCs) and there is immense scope of utilizing such MSCs for TE and other clinical applications.

In this investigation, GOnPs-impregnated biomimetic PCL and PLGA matrices were prepared with GO concentration within nontoxicity limit for human cells (≤50/ml [15]) for the fabrication of fibrous scaffolds by electrospinning technique. The widely used PCL and PLGA were chosen as the polymer matrices because of their low percolation threshold limit ($f_c \sim 0.80$ wt% GO) forming homogeneous composites with GOnPs as filler [16]. So far, very little work [6, 10] has been done for the direct differentiation and proliferation of human umbilical cord blood derived mesenchymal stem cells (CB-hMSCs) on pure biopolymer scaffolds or graphene oxide (GO)-polymer based composites scaffolds. The use of such biocompatible GO-PCL or GO-PLGA composite meshes for the myoblast differentiation of CB-hMSCs and oriented myotube formations are novel and challenging with immense future prospects of *in-vivo* tissue regeneration. The confirmation of myoblast differentiation of CB-hMSCs and oriented myotubes formation on GO-polymer electrospun meshes would also be advantageous for the next generation TE applications using such antibacterial biocompatible GO-polymer meshes. Since both PCL and PLGA-graphene oxide nonocomposite meshes exhibited excellent myoblast differentiation potential, in the present chapter, we shall mainly concentrate our discussion on the GOnPs-PCl composite system.

## 2. Synthesis of graphene oxide polymer composites for electrospinning

Graphenene oxide (GO) nanoplatelets (GOnPs), prepared from graphite powder [6], from homogeneous composites with many bioactive polymers like PVA, PCL, PLGA, chitosan, etc. [16] in DMSO, chloroform and many other solvents. Electrospinning is a unique technique for the preparation polymer nanofibres with diameters several micrometres to less than 50 nm. The electrospun scaffolds for the present study were prepared with GOnPs concentration 30 μg/ml solution as graphene oxide is non-toxic for human cell for its concentration below 50 μg/ml [15]. The electrospinning voltage was kept between 25 and 30 kV.

## 3. Characterization of GOnPs-polymer composite electrospun scaffold meshes

Electrospun GO-polymer (like PCL, PLGA or PVA) composite scaffolds showed enhancement of conductivity (σ) dielectric constant (ε) with their threshold values around 0.85 and 0.75wt% of GOnPs , respectively , for the case of GO-PCL (**Figure 1**) and GO-PLGA.

Figure 2a showed the well dispersed GOnPs solution, spin-coated GO film and sheet (prepared from pure GOnPs water solution). **Figure 2b** showed the characteristic GO peak appearing at $2\theta = 11.1°$, corresponding to a lattice *d*-spacing of 0.78 nm. For the GO-PCL or GO-PLGA meshes, an XRD peak (**Figure 2c**) appeared at 21.65° representing the crystalline phase of the polymer with no peak for GO around $2\theta = 11.1°$. The absence of GO peak was also reported

earlier in case of GO-PVA composite [17] which indicated disappearance of the regular and periodic structure of graphene oxide, the formation of fully exfoliated structures, and the homogeneous distribution of GOnPs in the polymer matrix [18].
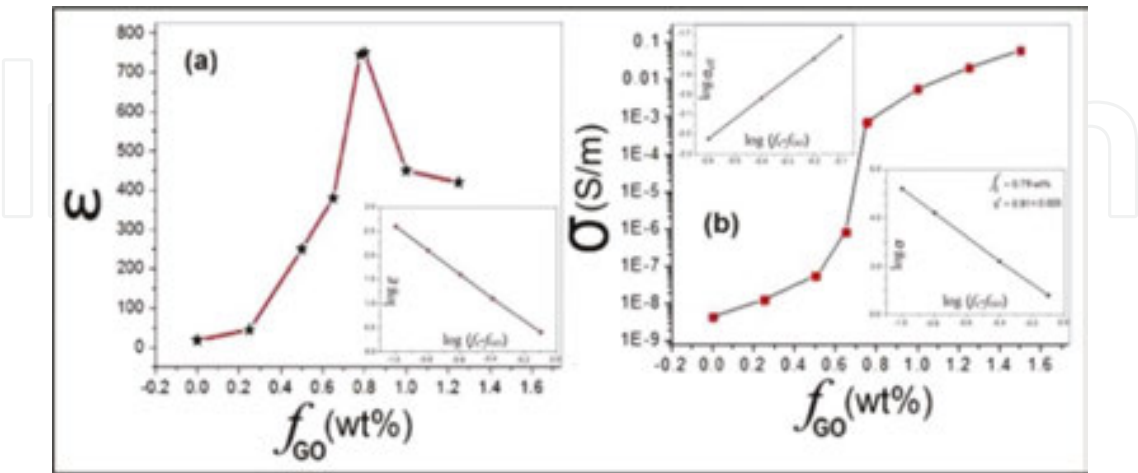
Figure 1. Dependence of (a) effective dielectric constant (ε) and (b) conductivity (σ) of the GO-PCL composite on GO concentration f_{GO}.
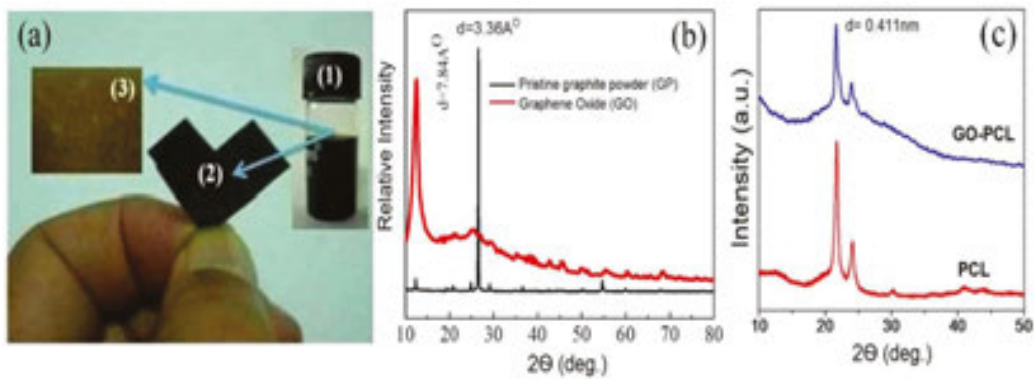

Figure 2. (a) Well dispersed GO-PCL solution (1), a free standing bendable tin GO sheet composed of GOnPs prepared by solution casting (2) which can be dispersed in water and spin coated GO sheet on cover glass (3) produced from GO solution. (b) The X-ray diffraction patterns of GO and pristine graphite powder, (c) GO-PCL and PCL, respectively.

The SEM micrograph of a GO sheet surface shown in **Figure 3a** indicated uniformly rough surface morphology. Inset of **Figure 3a** also presented FESEM micrograph showing the surface morphology of thin GO sheet which indicated wrinkles stacked in multiple GOnPs layers which favoured cell proliferation.

Figure 3b represented the SEM micrograph of the electrospun fibrous meshes and the selected area electron diffraction (SAED) pattern (inset of **Figure 3b**) with (average fibre diameter of 490 ±125 nm and porosity ~80–85%. **Figure 3c** presented the FESEM micrograph showing morphology of the broken edge of a GO sheet and inset of **Figure 3c** showed the HR TEM image of a single layer of the GOnPs film.
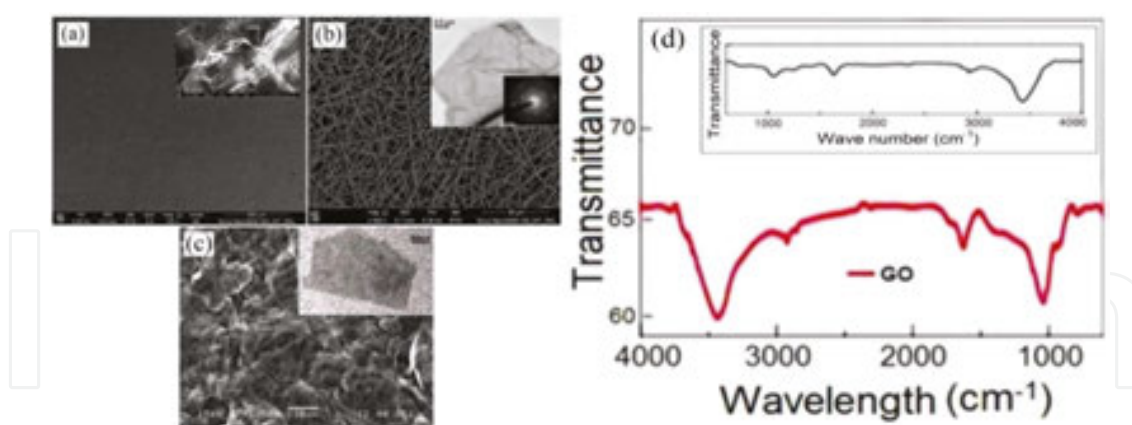
Figure 3. (a) SEM micrograph showing surface morphology of thin GO sheet (inset shows the FESEM micrographs of a particular portion the surface). (b) SEM micrograph of the GO-PCL electrospun meshes (inset shows the HRTEM image of GO present in GO-PCL along with the selected area electron diffraction (SAED) image). (c) FESEM micrographs of a broken edge of thin GO sheet (inset shows the HRTEM image of a single layer GO film). (d) FTIR spectra of GO sheets and pristine graphite powder (inset) distinguishing the behaviour of graphene and graphite powder. In GO intense bond around 3438 cm^{-1} corresponding to O–H band of CO–H is observed [6].

Raman is the vibration spectroscopic technique used to characterize GOnPs and identify the presence of GO in GO-PCL composite. Raman spectra of GO sheet as shown in **Figure 4a**, indicated the characteristic feature of GO peaks at frequencies around 1345 and 1597 cm^{-1}, respectively, for the G and D band usually assigned to the E_{2g} phonon of Csp^2 atoms and a phonon breathing mode of symmetry A_{1g}. Far infra-red (FTIR) spectra of GO and pristine graphite powder were shown in **Figure 4b**. The intense band at 3438 cm^{-1} is attributed to the O–H band of CO–H. The band at 1639 cm^{-1} is associated with the stretching of the C=O bond of carbonyl and carboxyl group.
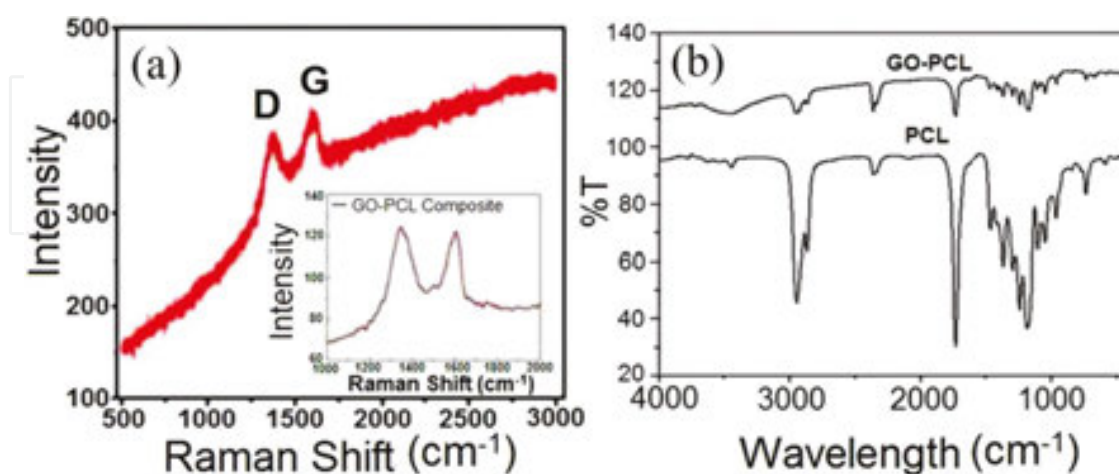
Figure 4. (a) Raman spectra of GO and GO-PCL composite meshes. (b) FTIR spectra of PCL and GO-PCL mesh distinguishing the behaviour of the two spectra. The spectra of GO-PCL if different from those of PCL and GO indicating strong coupling of GO and the PCL polymer. GO-PCL showed absorption bands at 1727 cm^{-1} indicating carbonyl stretching [20].

Deformation of the C–O bans is observed at the band present at 1070 cm^{-1}. FTIR spectra (**Figure 4b**) of GO-PCL showed absorption bands at 1727 cm^{-1} indicating carbonyl stretching. The bands appearing at 1295 and 1240 cm^{-1} represented the C–O and C–C stretching bonds [19]. The bands at 1239 and 1175 cm^{-1} were comparable with the asymmetric C–O–C stretching bonds indicating characteristic absorption [6] of PCL and strong interaction between GOnPs and polymer matrises.

Figure 5 indicates electrospun GO-PCL composite meshes which degrade up to ~16% in PBS (phosphate buffer saline) solution whereas electrospun PCL meshes degrade ~9% after 30 days of time interval. GO-PCL composite mesh showed optimized degradability rate that is suitable for cellular growth. Hydrophilicity of the GO sheet and GO-PCL composites were measured by contact angle measurement. Wetting (CA$_w$) and dewetting (CA$_{dw}$) contact angles of thin GO sheet and GO-PCL mesh films are shown in **Figure 5** (inset). In case of thin GO sheets, CA$_w$ was found to be around ~58.7° with hysteresis (CA$_w$–CA$_{dw}$) of ~4° which might be a measure of the solid-liquid interaction [6, 20].
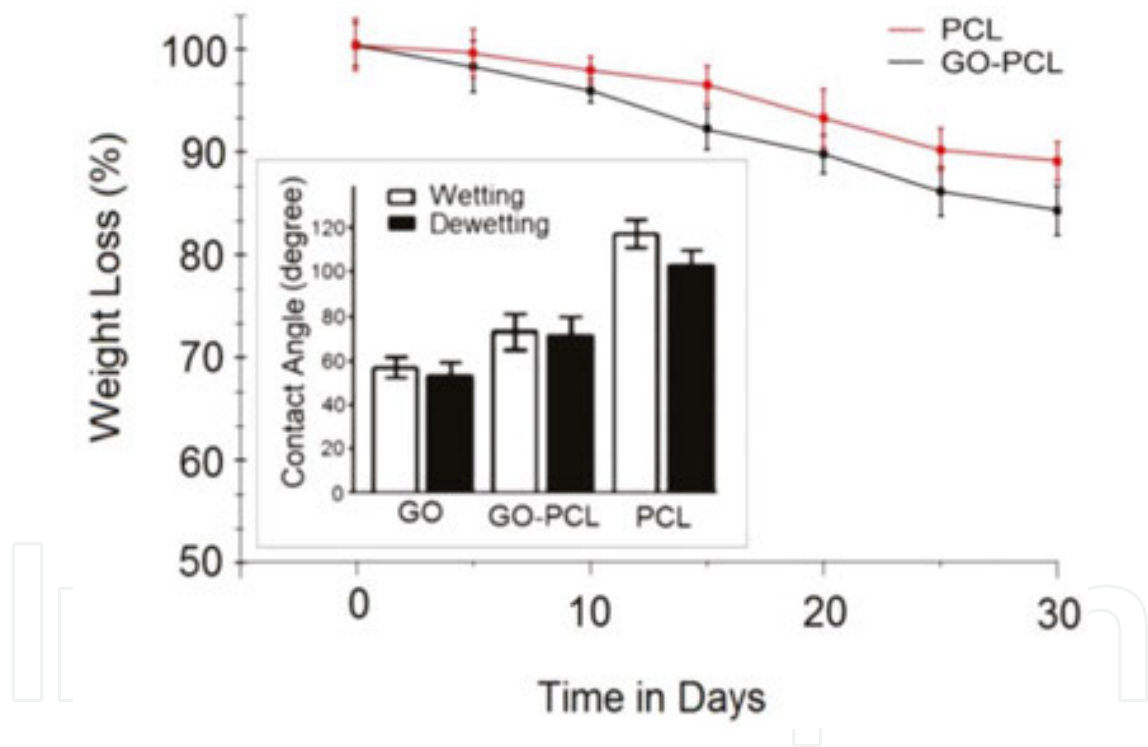

Figure 5. *In-vitro* degradation pattern of electrospun PCL and GO-PCL composite scaffolds in PBS(phosphate-buffer solution) for 30 days. Inset shows contact angle analysis (in degrees) representing both advancing (wetting) and receding (dewetting) water sessile drop on GO sheets, GO-PCL and PCL meshes. Error bars present standard deviation.

The stress-strain curves of GO sheets and GO-PCL meshes were shown in **Figure 6**. The tensile strength of PCL (~1.88 ± 0.25 MPa) was found to increase significantly with addition of GO (~4.8 ± 0.25 MPa). The tensile strength is also known to increase with increasing GO concentration. Favourable mechanical property supported GO-PCL and GO-PLGA meshes for tissue engineering applications.
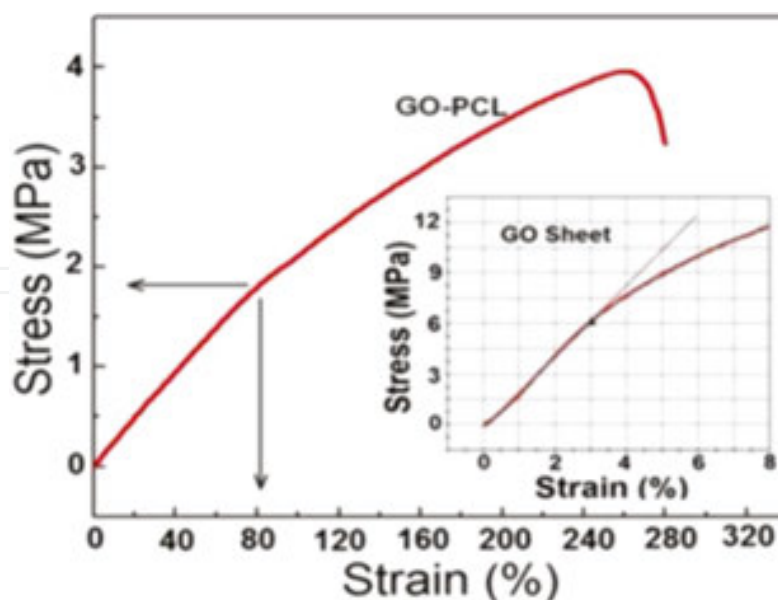
Figure 6. The stress-strain curve of the GO sheet and GO-PCL meshes carried out at RT with GO concentration within the non-toxic limit (~20 μg/ml) [6].

As shown in **Figure 7**, GO added PCL (GO-PCL composite) exhibited appreciably large increase of both ε (~300 for GO-PCL and only ~25 for PCL) and σ (>2 orders of magnitude higher in GO-PCL compared to that of GO sheet). Similar enhancement of σ and ε was also observed in GO-polyvinyl alcohol (PVA) and other GO-polymer composites [6, 17].
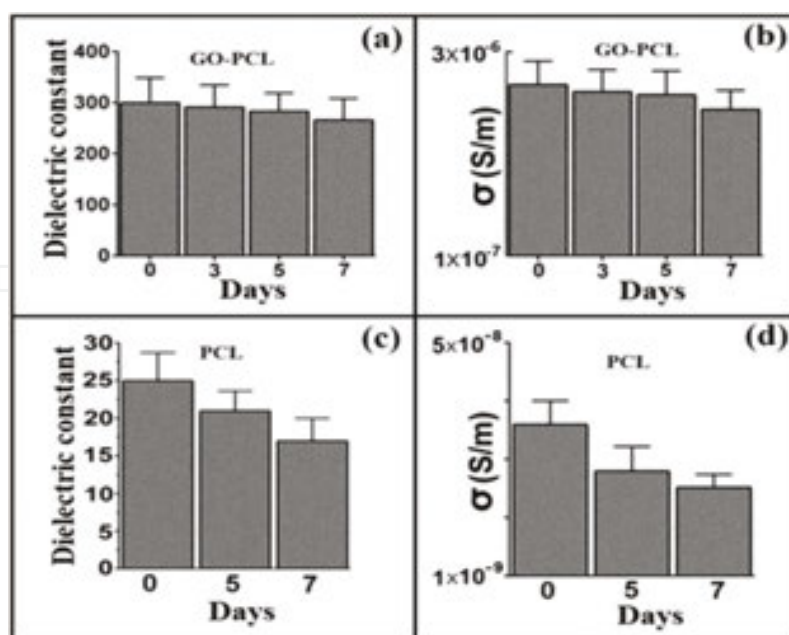
Figure 7. (a) Room temperature (RT) dielectric constant (ε) and (b) conductivity (σ) data of GO-PCL meshes before (0 days) and after immersion in PBS solution for up to 7 days. RT ε (c) and σ (d) data of PCL meshes before (indicated by the 0 days) and after immersion in PBS solution (all measurements were performed 1 kHz).

Similar conductivity and dielectric constant behaviour (shown in **Figure 7**) was also observed in case of GOnPs-PLGA meshes soaked in PBS solution. In this case, enhancement of conductivity is little lower than those of GOnPs-PCL scaffold meshes indicating little lower biocompatibility of the GOnPs-PLGA composite.

4. *In-vitro* cell culture study

### 4.1. Isolation and culture of mononuclear cells from UCB

The mononuclear stem cells (MNCs) were isolated from UCB (**Figure 8a**). Morphology of MNCs was initially round shaped (after 48 h of culture) shown in **Figure 10b** via phase contrast microscope.
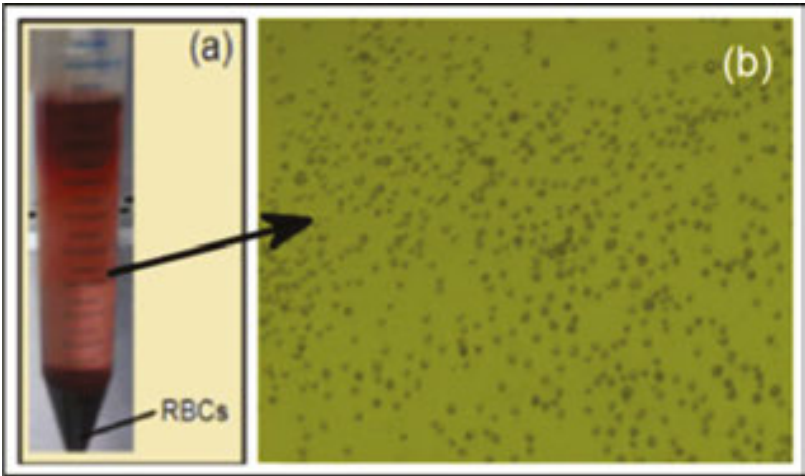
Figure 8. (a) Mononuclear cells (MNCs) layer (middle) and red blood cells (RBCs) precipitated at the bottom in a 50 ml culture tube. (b) Isolation of MNCs being cultured in a cell culture plate.
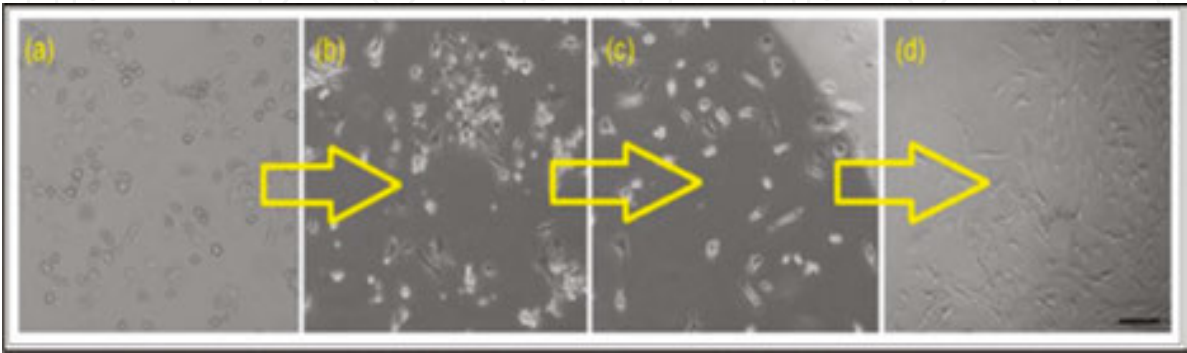
Figure 9. Gradual morphological changes of umbilical cord blood derived mesenchymal stem cells (MSCs). After fifth passaging fibroblast like morphology (d) of the cultured cells were observed under phase contrast microscope. Scale bar: 50 μm.
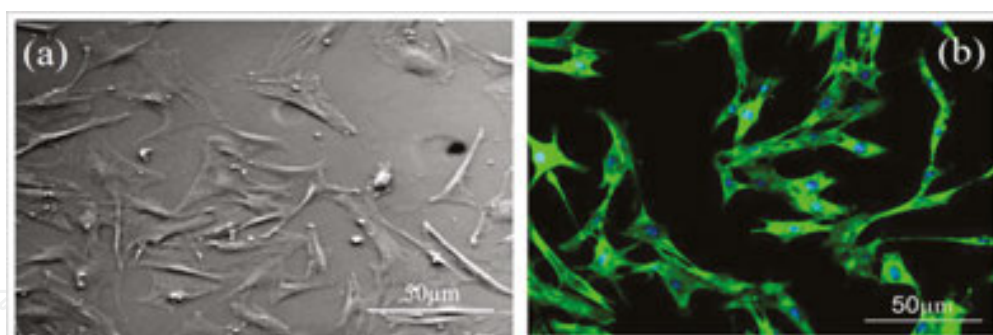
Figure 10. Morphology of MSCs analysed using phase contrast microscope (a) and (b) cytoskeleton staining of actin filaments along with nuclei counterstained with DAPI (fluorescence image).

4.2. Isolation of UCB-derived MNCs

UCB samples were diluted with DMEM media in the ratio of 4:1 before use. The mononuclear cells (MNCs) were isolated [20] using the Ficoll Hypaque (Histopaque-1077; Sigma, MO, USA) density gradient centrifugation (with swinging-bucket rotor) at 450 g for 30 min. The erythrocytes were lyzed by incubating with 1% lysis buffer for 10 min and spinning at 200 g for 10 min. The pellet thus obtained was washed twice with phosphate-buffer saline (PBS) by centrifuging at 200 g for 10 min. Finally, the pellet obtained were culture in DMEM, 10% foetal bovine serum, 1% antibiotic with addition of 10 ng/ml basic fibroblast growth factor (bFGF). Initial media was changed after one day to remove the RBC and cell derbies after that media change after 3-day interval. Cells were then cultured for up to fifth passage.

4.3. Characterization of UCB-derived MSCs by flow cytometry

Cells were analysed by fluorescence-activated cell sorting (FACS) method. In brief, cells were trypsinized and washed with fluorescence activated cell sorting (BDFACS) buffer. After centrifugation at 200 g for 5 min at 4°C, cells were suspended in PBS at a concentration of 1×10^5 cells/ml and repeatedly washed to remove phenol red contained in the media. The cells were finally suspended in 100 μl of FACS buffer. Cells were then labelled with CD90-FITC, CD73-PE, CD105-APC, CD45-PE, CD34-FITC and HLA DR-APC monoclonal antibodies at 4°C for 30 min in the dark. The labelled cells were then analysed by flow cytometry (BDFACS Fortessa II) with at least 10,000 cells being acquired and analysed.

4.4. Morphological characterization of CB-hMSCs

The morphological variation in the cultured cells was studied by phase contrast microscopic images (**Figure 9**). After initial culture, cells were round/spherical shaped during the initial days of culture and became elongated as spindle fibroblastic shape gradually (**Figure 9a–d**) after fifth passage.

The morphology of cells was also analysed using cytoskeleton staining of actin filaments (**Figure 10**). Cells (stained with FITC-phalloidin) were observed under a Zeiss Axivert 40 CFL fluorescence microscope.

4.5. Immunophenotypic characterization of CB-hMSCs

The immunophenotypic characterizations are shown (**Figure 11**) to be positive for CD90 (99.2%), CD73(98.5%), CD105 (98%) and negligible for hematopoietic markers like CD45 (1.5%), CD45 (0.5%) and HLA-DR (1.0%) indicating mesenchymal stem cells phenotype. Similar behaviour was also exhibited by the GO-PLGA meshes [20].
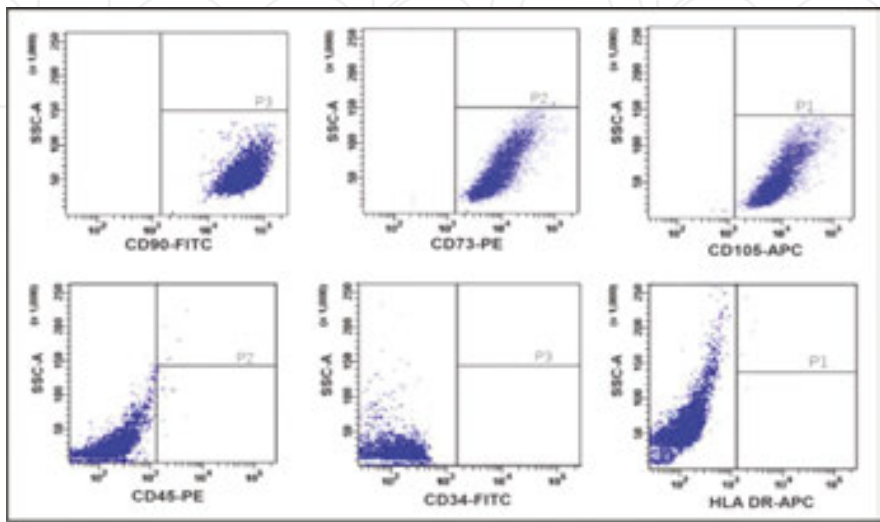

Figure 11. The immunophenotypic analysis was found to be positive for CD90 (99.2%), CD73 (98.5%), CD105 (98%) and negative for CD45 (1.5%), CD34 (0.5%) and HLA-DR (1.0%) indicating mesenchymal stem cells phenotype.

4.6. Cell metabolic activity

WST-8 assay was used to study the metabolic activity of the MSCs on the prepared scaffolds on various time intervals. The cellular viability of metabolic activity of the cultured MSCs on
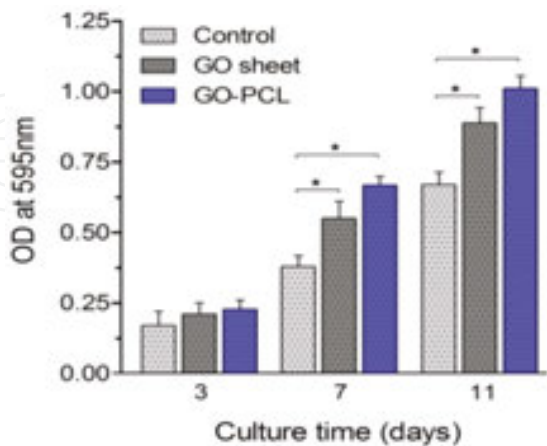

Figure 12. WST-8 assay of CB-hMSCs grown on GO sheet, GO-PCL and control (tissue culture plate) substrates after 3, 7 and 11 days of culture. Superior cellular metabolic activity has been observed on GO-PCL-based composite meshes. Results presented as the means ± SD. * indicates significant difference ($n = 5$; $p < 0.05$). Metabolic activity was increased with time with the scaffolds showing the trend GO-PCL > GO > control substrate.

the prepared GO-based scaffold was further evaluated quantitatively by WST-8 assay as shown in **Figure 12**.

4.7. Cell proliferation assay (via DNA quantification)

The proliferation of MSCs on the prepared scaffolds was evaluated by DNA quantification assay. **Figure 13** shows an increasing rate in DNA content of MSCs with time as observed in different GO-based substrates prepared for investigation.
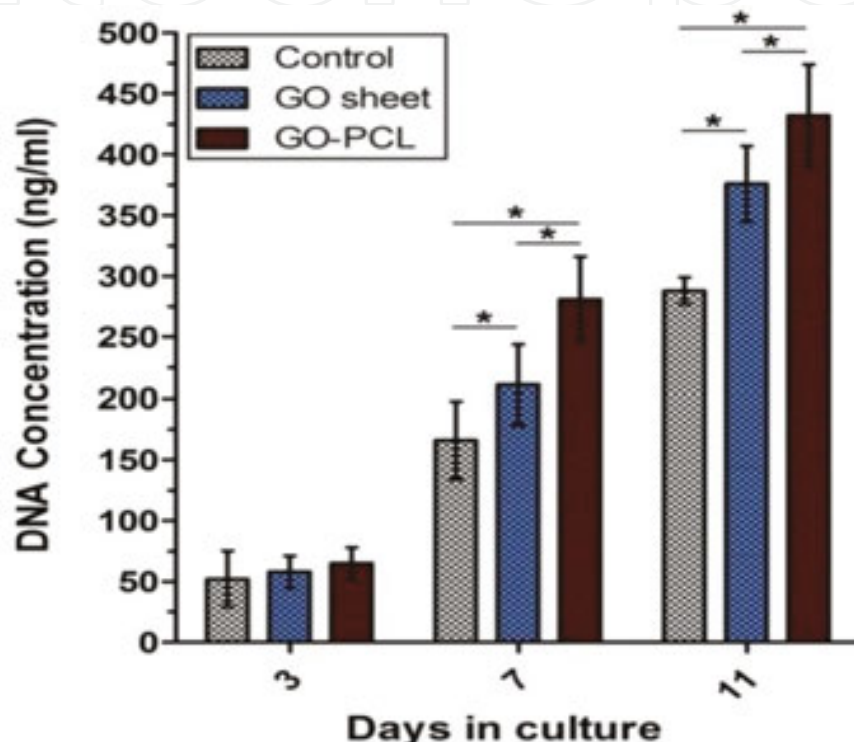

Figure 13. Cell proliferation represented in terms of DNA quantification on GO sheet, GO-PCL mesh and control (tissue culture plate) substrates. An increased trend in DNA content is observed on all the GO-based matrixes. Results represented as mean ± SD, * indicates significant difference ($n = 5$; $p < 0.05$).Proliferation of MSCs were increased with time with the scaffolds showing the trend GO-PCL > GO > control substrate.

The corresponding DNA contents of hMSCs cultured on tissue culture plate (TCP) was taken as control, GO sheet and GO-PCL composite meshes on 3–11 days of culture are ~50 to ~285, ~58 to ~375 and ~65 to ~430 ng/ml, respectively.

4.8. MSCs seeding, attachment and spreading

After seeding of MSCs (by static seeding method with ~2×10^4 cells/ml), attachment and spreading of these cells was evaluated by scanning electron microscopic (SEM) micrographs on increasing time interval (**Figure 14**). Cellular attachment and spreading rate also indicates their compatibility to the scaffold environment.
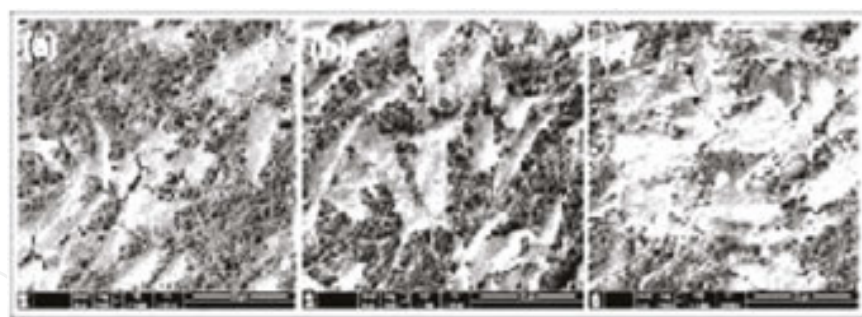
Figure 14. Attachment and spreading of CB-hMSCs on GO-PCL composite scaffolds on days 3 (a), 5 (b) and 7 (c) of culture. The MSCs are well visualized from the micrographs.

4.9. Differentiation potential of CB-hMSCs on GO-PCL composite meshes

4.9.1. Myoblast differentiation potential

After confirming viability and proliferation of cord blood derived mesenchymal stem cells (CB-hMSCs or simply MSCs) onto the novel GO-PCL composite scaffolds, MSCs were further allowed for myoblast differentiation on these substrates. Along with differentiation of MSCs, elongated bipolar morphology of myoblasts have been observed as seen from FESEM micrographs (**Figure 15a** and **b**).
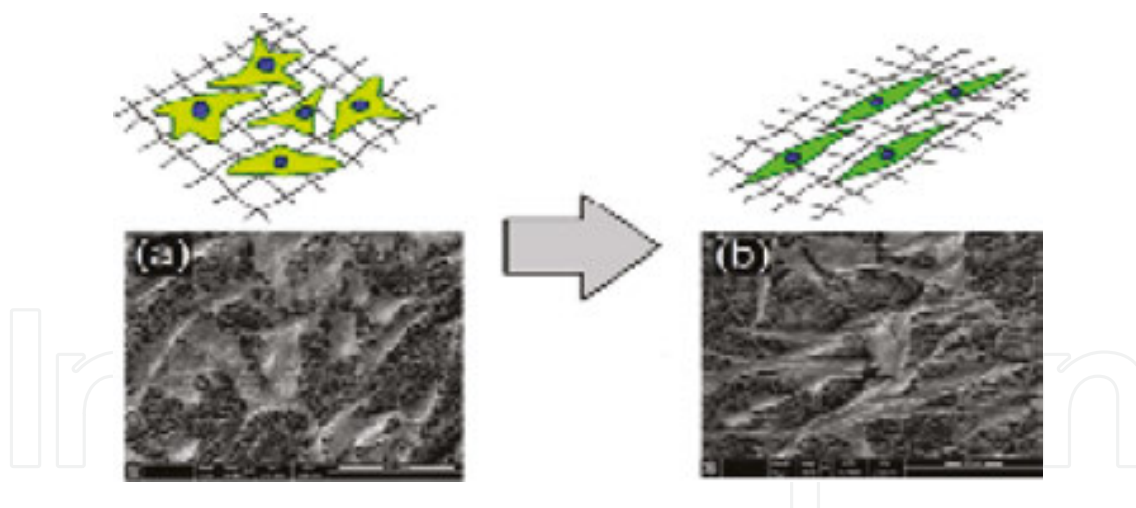
Figure 15. Morphology of CB-MSCs (a) changes towards bipolar structure (b), same as myoblasts, on GO-PCL electrospun composite scaffold that indicates differentiation of MSCs to myoblast cells (morphology wise).

4.9.2. Myoblast viability and proliferation
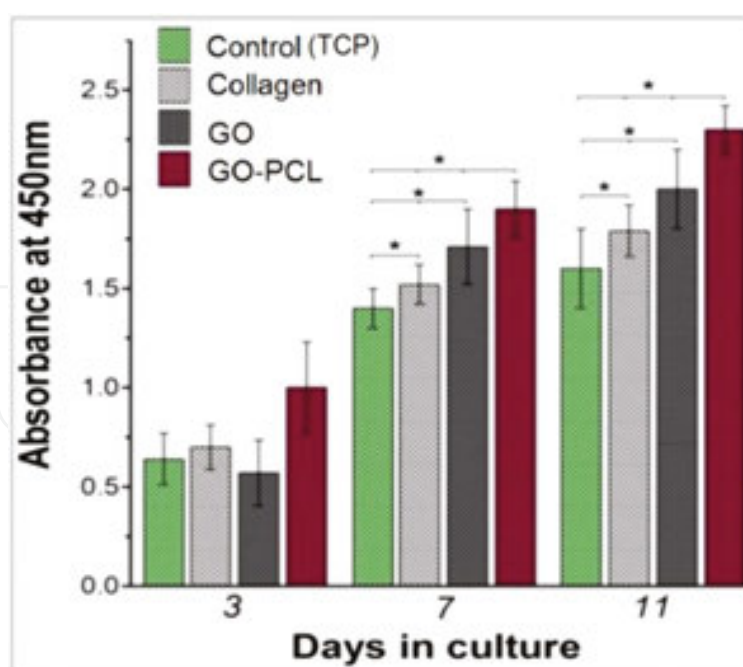
4.9.2.1. Cell viability and proliferation assay

The vastly used methyl thiazolyl diphenyl-tetrazolium bromide (MTT) assay which is a typical nontoxicity assay may not correctly predict the toxicity of GO because of the mild reaction of

MTT salt with GO resulting in an incorrect positive signal. Therefore, we used, alternatively, a water soluble tetrazolium salt (WST-8) assay. Cell viability and proliferation on GO/PCL composite meshes, thin GO sheet and controls were measured by water-soluble tetrazolium salt (WST-8) assay after 3, 7and 11 days of cell seeding in 96-well culture plate. Ten microlitre of cell proliferation reagent (WST-8) was added into each well containing sample with 100 μl of culture medium and incubated for 4 h at 37°C. Absorbance (OD) of the solution was then measured at 450 nm by a microplate reader (Varioskan Flash, Thermo Scientific). The cells seeded on collagen scaffolds were evaluated as control. WST-8 was reduced by dehydrogenase activities of living cells that give rise yellow-colour formazan dye. The amount of formazan dye generated (by the activities of dehydrogenases) was directly proportional to the number of living cells.

4.9.2.2. Evaluation of myotubes formation

For immunostaining analysis, human skeletal myoblast cells (hSkMCs) grown after 5 days of culture on different substrates (i.e. collagen and glass controls, GO sheets and GO-PCL meshes) were analysed for the expression of myogenin, an early myogenic differentiation marker. Briefly, to detect myogenin, cells were fixed and incubated with primary antibody (1:100) at 4°C overnight and after washed with PBS, again incubated with secondary antibody DyLight 488-conjugated goat anti-mouse IgG (1:100) at RT for 1 h. before viewing. On 11 days of culture, cells were analysed for further expression of muscle specific antigens such as myosin heavy chain (MHC) and dystrophin. Cells were fixed with 4% paraformaldehyde, permeabilized with
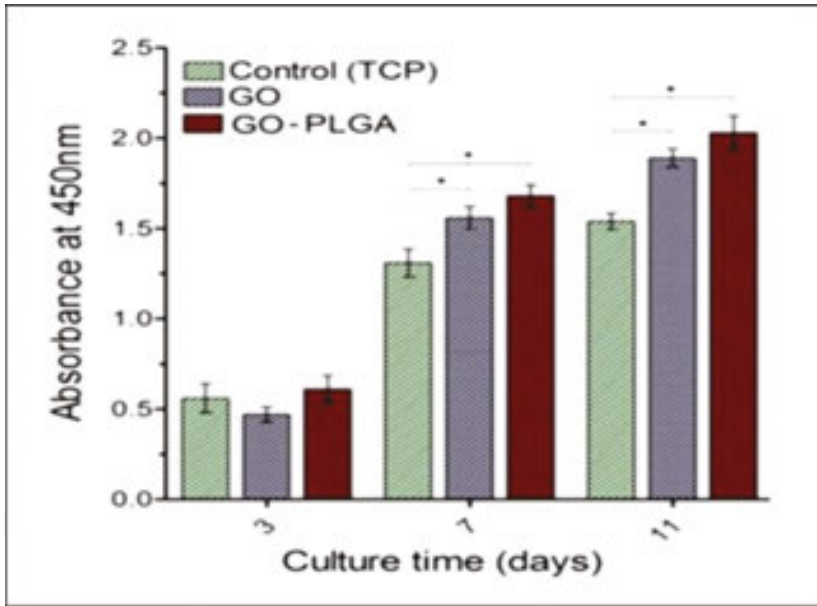

Figure 16. Viability and proliferation of myoblasts observed bytetrazolium salt (WST-8) assay. Superior viability of cells has been found on GO-PCL composite meshes compare to GO sheet and other controls (collagen and tissue culture plate) indicating better myoblast differentiation potential and hence biocompatibility. Results presented as the means ± standard deviation. * indicates significant difference ($n = 5$; $p < 0.05$).

0.1% Triton X-100, and then incubated in goat polyclonal anti-MHC (1:100) and rabbit poly-clonal anti-dystrophin (1:100) as primary antibodies for 1 h. Next, after washing with PBS, a FITC conjugate rabbit anti-goat secondary antibody (1:500) was used to detect MHC, while Texas Red conjugated goat anti-rabbit secondary antibody (1:150) was also employed to detect dystrophin. Both MHC and Dystrophin are myotubes-specific markers. The samples stained without primary antibody served as negative controls. Nuclei were counterstained with 4′,6-diamidino-2-phenylindole (DAPI). Substrates with cells were then mounted for fluorescence microscopic studies using a Zeiss Axivert 40 CFL fluorescence microscope.

Figure 16 shows viability and proliferation of myoblast cells on GO sheets, GO-PCL mesh and controls. Cell viability (from WST-8 assay analysis) was found to increase significantly for GO sheets and GO-PCL meshes compared to the control surfaces (*$p < 0.05$).

This was ascribed to be due to the better myogenic differential potential contributed by the favourable physicochemical properties of graphene oxide. This result implied that GO sheets and GO-PCL meshes were cytocompatible and supported cell viability that increased the biocompatibility of GO-PCL composite scaffolds.


Figure 17. Myoblast cells viability and proliferation observed by tetrazolium salt (WST-8) assay. Results presented as mean ± standard deviation. * indicates significant difference ($n = 5$, $p < 0.05$). Viability was found to increase with time on the samples showing the trend of GO-PLGA > GO > control substrate (tissue culture plate).

The viability of myoblast cells on GO-PLGA composite scaffolds were also analysed by WST-8 assay. **Figure 17** showed the viability of GO-PLGA mesh along with control and GO sheet (for comparison). Cell viability was found to increase significantly on GO sheets and GO-PLGA meshes compared to that on the control surfaces (*$p < 0.05$). This result implies that GO-PLGA mesh is cytocompatible and supported myoblast proliferation as in the case of GO-PCL composite meshes. It is thus seen that electrospun GO-polymer meshes with low

GO concentration (not toxic to human cells) provided favourable circumstance for the growth and proliferation of myoblast cells.

### 4.9.3. Immunophenotypic characterization of myoblast cells

Flow cytometric analysis of cells adhered on thin GO sheets and GO-PCL meshes was performed to confirm the positive expression of myogenic markers CD56 and desmin indicating skeletal muscle cell phenotype (**Figure 18**).
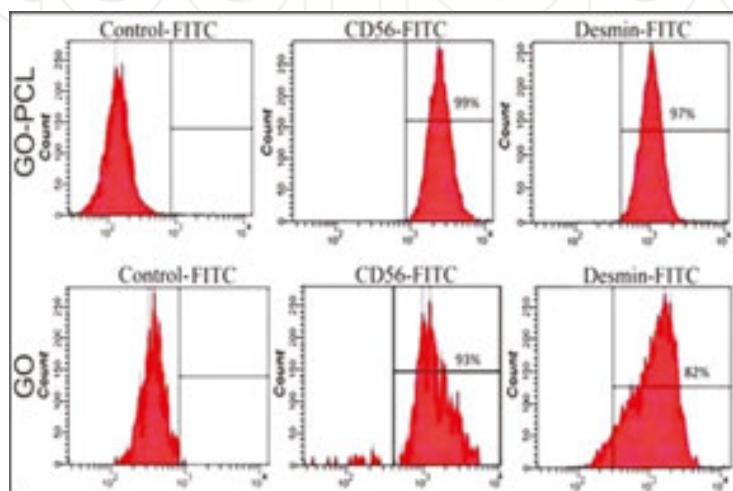
Figure 18. FACS analysis of trypsinized hSkMCs from GO-PCL meshes and GO sheets after 7 days of culture. Cells were highly expressed for skeletal muscle markers CD56 and desmin indicating myoblast cells phenotype.

4.9.4. Aspect ratio analysis

After 3 days of culture, the aspect ratios measured on GO-PCL meshes, GO sheets and controls were found to be ~6.6, ~5.4 and (~4.7 for collagen mesh and ~4.3 for tissue culture plate (TCP)), respectively (**Figure 19**).
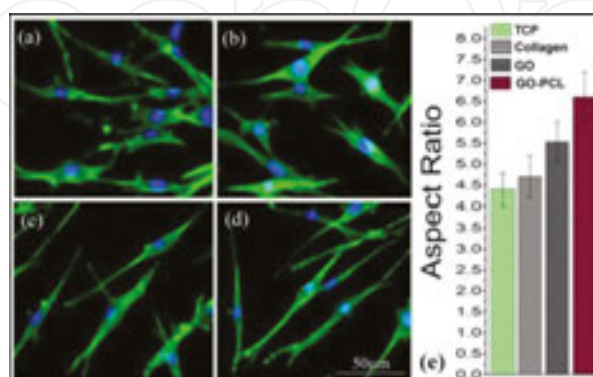
Figure 19. Analysis of cytoskeleton development of hSkMCs grown on (a) control (tissue culture plate (TCP)), (b) collagen mesh, (c) GO sheets, (d) GO-PCL meshes. (e) Cell aspect ratio quantification from (a) to (d) after 3 days of culture. Increased aspect ratio indicates better elongation of these cells on GO-based substrates.

4.9.5. Formation of myotubes

The myoblast cells were bipolar at the initial stage (**Figure 20a** and **b**) and they were fused together on extended time interval (day 11) under proper condition and formed myotubes that were further clarified by FESEM micrograph (**Figure 20c**) as well as immunostaining assay (**Figure 20d–l**). These figures showed improved myoblasts cell proliferation, differentiation and formation of myotubes onto GO-PCL meshes compared to GO-sheet and control.
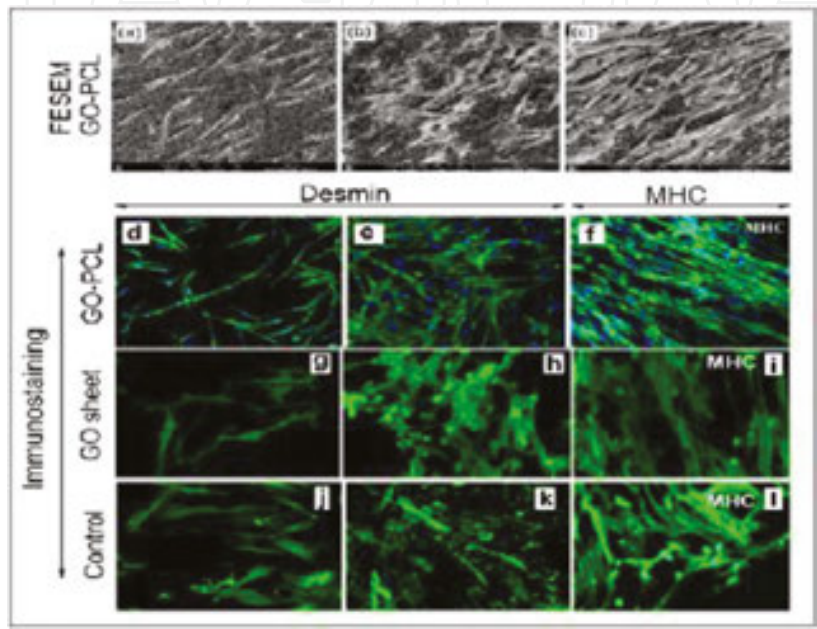
Figure 20. FESEM micrographs of GO-PCL electrospun scaffolds representing cells attachment as well as spreading at increasing time interval (day 3 (a)–day 7 (b)) and also formation of myotubes at extended time of differentiation (day 11 (c)). For better comparison, immunostaining (with desmin-FITC and MHC-FITC conjugated) images of the corresponding FESEM images have also been shown alongside (d–l) with GO sheet and control (tissue culture plate (TCP)) substrate [6, 19].

4.9.6. Immunohistochemical characterization

This process has widely been used for the detection of cells specific antigens (proteins, e.g. desmin, MyoD, Myosin Heavy Chain, Dystrophin, etc.) to verify the presence of specific cells/ tissues. Immunohistochemical analysis (**Figure 21a–l**), along with FESEM analysis of the corresponding samples (**Figure 21m–p**), confirmed differentiation of CB-hMSCs to myoblasts via early expression of myogenin-positive nuclei on controls, GO sheet and GO-PCL mesh (**Figure 21a–d**).

Moreover, muscle-specific antigens like myosin heavy chain (MHC) shown in **Figure 22e–h** and dystrophin (**Figure 21i–l**) were expressed more intensely on GO-PCL meshes compared to those on thin GO sheets or control substrates. Myotubes formed on GO sheets and GO-PCL meshes were found to be more aligned compared to those on the control substrates. Quantitative analysis of the percentage of myogenin-positive nuclei showed in **Figure 21** that myogenin expression increased more on thin GO sheets and GO-PCL meshes compared to

that on control substrates (collagen mesh and tissue culture plate), which also indicated a better differentiation potential of the GO-based substrates. Importantly, GO-PCL meshes showed the highest percentage of myogenin positive nuclei (~19%) (**Figure 21**). Significantly higher expression of early myogenic marker (myogenin) indicated superior myogenic differentiation potential of GO-PCL electrospun meshes compared to GO sheets and controls.
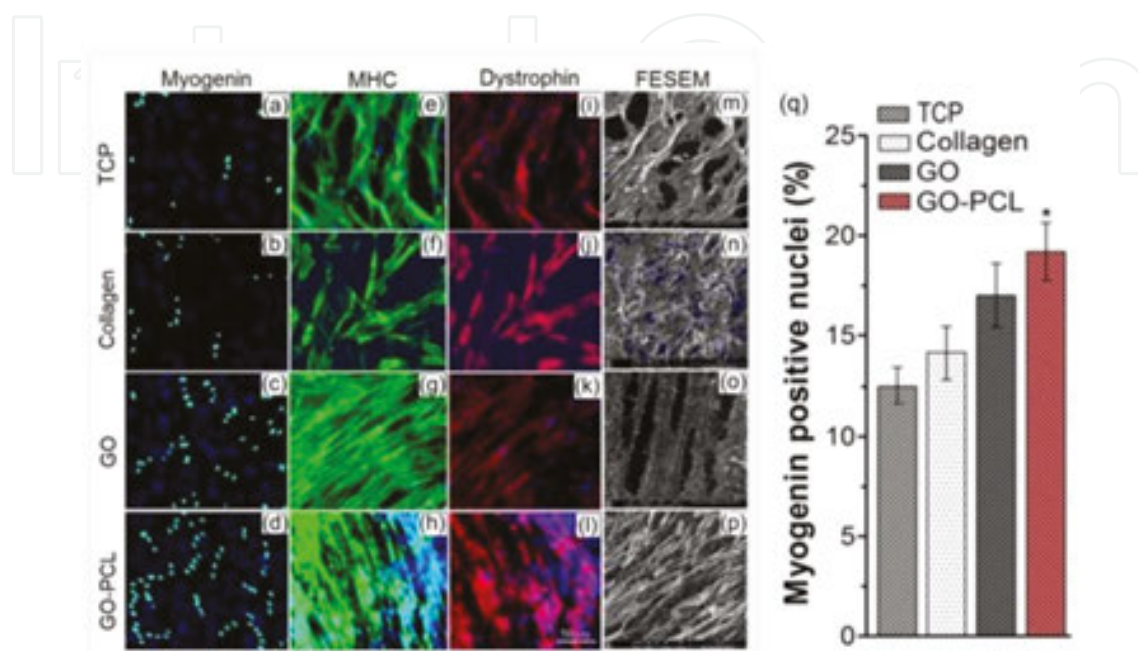

Figure 21. Expression of the early myogenic differentiation marker myogenin-positive nuclei (green) on controls (a and b), GO sheets (c) and GO-PCL meshes (d). Immunostaining of MHC (green), respectively, on controls (collagen and tissue culture plate) (e and f), GO sheets (g) and GO-PCL meshes (h) and dystrophin (red) similarly on controls (i and j), GO sheets (k) and GO-PCL meshes (l). Nuclei were counterstained with DAPI.FESEM micrographs (m–p) of the corresponding samples were also shown for better demonstration (q). Quantitative analysis of percentage myogenin-positive nuclei (cells cultured in differentiation medium for 5 days before staining). * represents significant difference ($p < 0.05$) compare to collagen mesh and tissue culture plate (TCP) taken as controls [6].

Similar to the GO-PCL composite meshes, immunohistochemical study has also been performed with myoblasts grown on electrospun GO-PLGA meshes. The experimental results confirmed the differentiation of CB-hMSCs into skeletal myoblasts by the expressions of desmin and MyoD, and formation of myotubes by the expression of MHC on GO-PLGA composite meshes and control (tissue culture plate) (**Figure 22**). Immunostaining of desmin and MyoD after 3–7 days of culture expressed almost similar on both control and GO-PLGA substrates. But, formation of MHC on GO-PLGA mesh was much better compare to control.

Formation of myotubes was also more aligned, similar to natural orientation. This indicates better myotubes formation hence better myogenic maturation potential of GO-PLGA mesh. But, GO-PCL composite meshes showed even superior myoblast proliferation as well as differentiation potential compare to GO-PLGA meshes. This might be due to the fact that PLGA released acidic byproducts upon its degradation that hamper cellular interaction. Moreover, conductivity of GO-PCL was also higher than that made GO-PLGA mesh that also makes GO-PCL more suitable for electro-responsive skeletal muscle tissue regeneration.
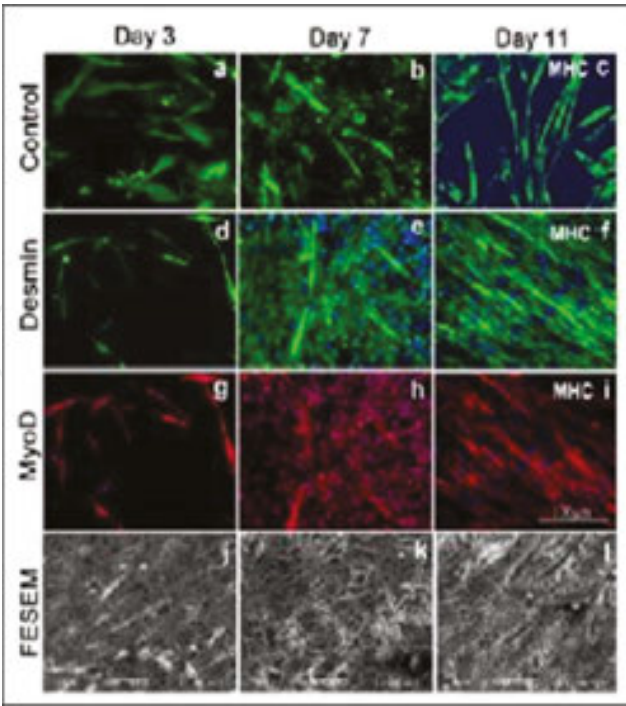
Figure 22. Immunostaining of desmin, MyoD and MHC (myosin heavy chain) on control (a–c) and GO-PLGA electro-spun composite mesh (d–i). Corresponding FESEM micrographs (j–l) of these samples were shown for better demonstration. It is revealed that though GO-PLGA showed better myoblast differentiation compared to that on GO sheet. GO-PCL exhibit superior myoblast differentiation and myotube formation compared to the GO-PLGA meshes [20].

5. Expression of myogenic protein and IGF-1 cell signalling pathway analysis

The ability of cells to correctly respond to their microenvironment is the basis of tissue repair and development [21, 22]. Here, myogenic protein expression on GO sheet and electrospun GO-PCL scaffolds and cell signalling pathway (insulin-like growth factor-1 (IGF-1)) analysis have been investigated. Better myogenic protein expression was observed on GO-based polymer composite representing superior myogenic differential potential. It was also observed that late myogenic protein, myosin heavy chain (MHC) related to the formation of myotubes, expressed more on GO-PCL composite scaffolds compare to GO sheet and control (tissue culture plate). Myogenic gene (desmin, MyoD and MHC) expression was also found to be better on GO based polymer composite substrate. In addition, IGF-1 pathway, important for skeletal muscle cells growth and maturation [23, 24], was also studied with various intermediate proteins (IRS-1/PI(3)K/Akt/MyoD) expression. Inhibition of Akt was investigated to examine the variation of the expression of myogenic protein MyoD, involved in skeletal muscle differentiation [24, 25]. The expression of MyoD was observed to reduce along with the inhibition of Akt that indicated effectiveness of IGF-1 pathway for skeletal muscle cells differentiation and maturation.
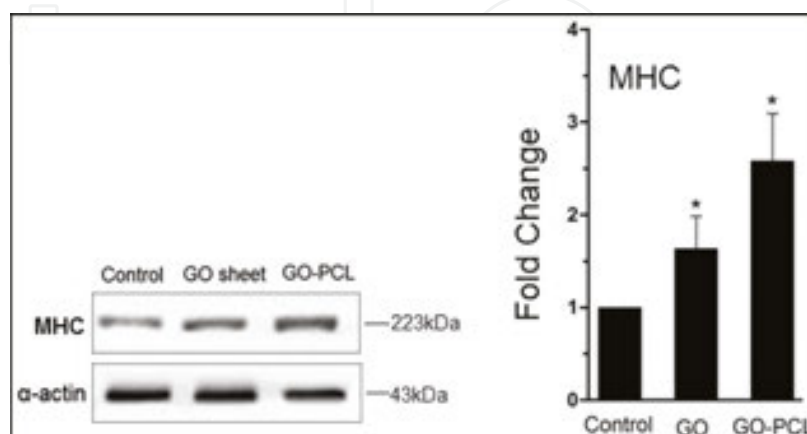
5.1. Expression of myogenic proteins

Expressions of myogenic proteins such as desmin, MyoD and MHC were assessed on GO-PCL meshes, GO sheet and control (tissue culture plate) using Western blot analysis. **Figure 25** showed expressions of desmin and MyoD on these substrates after 5 days of culture. Both of these proteins expressed well on GO-based substrates. The electroconducting GO-PCL composite mesh showed the highest expression due to better interconnectivity that enhanced cellular growth and hence their protein expressions.
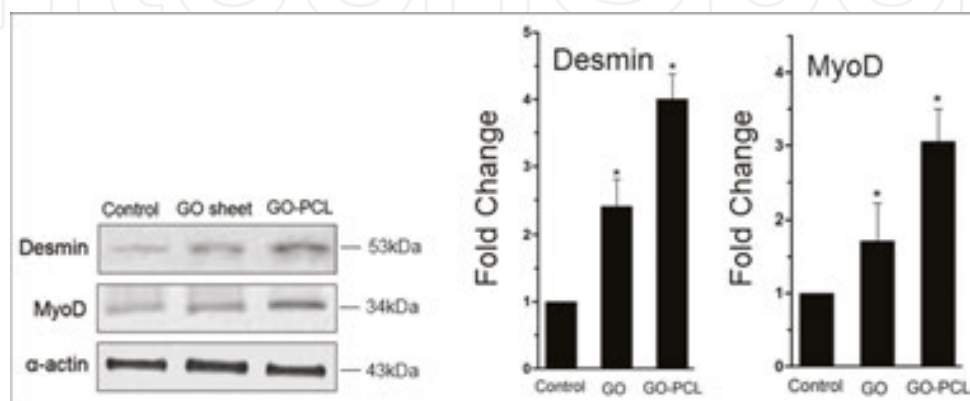
Figure 23. Expression of myogenic protein desmin and MyoD (left) and expression of fold change on GO-PCL mesh, GO sheet and control (tissue culture plate) (right) for the corresponding proteins. * indicates significant difference compare to control ($p < 0.05$).

From the present observation (**Figure 23**), the expression levels of desmin and MyoD proteins were found to be enhanced on grapheme-based scaffolds, compared with to that of control as follows: 2.4-fold on GO, 4-fold on GO-PCL for desmin and 1.8-fold on GO, 3.1-fold for GO-PCL for MyoD. Data reported as fold change from control (means ± SE). *indicates significant differences ($n = 5$; $p < 0.05$).

Figure 24. Expression of myogenic protein (MHC) (left) and expression of fold change on control, GO and GO-PCL substrates (right). * indicates significant difference from control ($p < 0.05$).

After 11 days of culture on the same substrates, expression of MHC (a late myogenic marker) was assessed using Western blot analysis (**Figure 24**). Expression of MHC, related to formation of myotubes was found to be better on GO and GO-PCL meshes compared to control substrate. Here, better expression of this protein in GO-PCL mesh also indicates better myotube formation on this substrate as described earlier (**Figure 23**).

The expression levels of MHC protein were found to enhance on GO-PCL composite and GO sheet compared with that of control: 1.6-fold on GO and 2.5-fold on GO-PCL mesh. Data were reported as fold change from control (means ± SE).
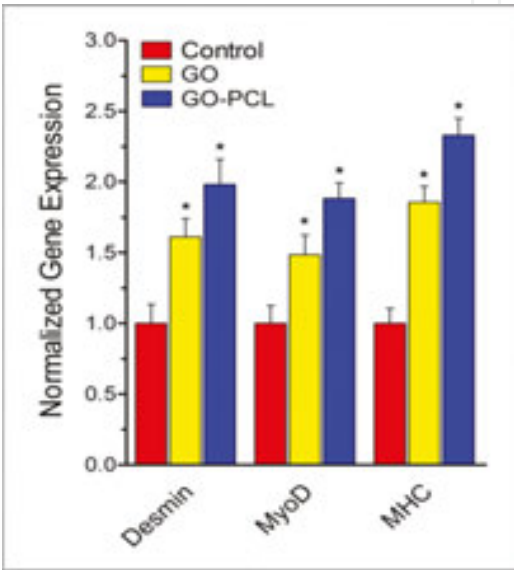
Figure 25. Expression of myogenic genes (desmin, MyoD and MHC) in myoblasts grown on electrospun GO-PCL mesh, GO sheet and control (tissue culture plate) substrates. * indicates significant difference from control ($p < 0.05$).

5.2. Myogenic gene expression

Real-time RT-PCR was used to analyse the expression level of MyoD, desmin and MHC on GO sheet, GO-PCL scaffolds and control. It was found, similar to protein expression, that these myogenic genes expressed better on GO-PCL composite and GO sheet.

Highest expression was found on myoblast cells grown on GO-PCL meshes. Quantitative RT-PCR analysis was performed after differentiation for 5 days for desmin and MyoD and 11 days for MHC (as MHC express late). As shown in **Figure 25**, the expression levels of all of the tested genes were enhanced on graphene derivative and GO-polymer composites, compared with that of the control as 1.60-fold on GO and 1.98-fold on GO-PCL for desmin; 1.48-fold on GO and 1.88-fold on GO-PCL for MyoD; 1.86-fold on GO and 2.33-fold on GO-PCL for MHC. * denotes a significant difference compared to control substrate.

Significant up-regulation of myogenic gene expression indicated that the GO-based substrates enhanced both early and late stages of myogenic differentiation, subsequently stimulating the formation of myotubes. In addition, higher expression of myogenic proteins and genes on GO-

PCL substrates again confirmed its superiority perhaps due to its higher conductivity and dielectric constant associated with GO surface charge.

5.3. Cell signalling pathway analysis

5.3.1. Insulin-like growth factor 1 (IGF-1) pathway study

IGF-1 is one of the most important pathways that have been studied extensively in the field of muscle growth [23, 24]. Researchers studied IGF-1/IRS-1/PI(3)K/Akt/MyoD pathway and concluded its importance for skeletal muscle differentiation and maturation [23–27]. In the present study, it was attempted to verify this pathway using the novel graphene based composite scaffolds (**Figure 26**). IGF-1 is one of the primary mediators of the effects of growth hormone (GH) in body that stimulates growth via growth promoting effects on almost every cell, especially muscle cells present in the body. IGF-1 is also capable of regulating cellular growth and development. In addition, IGF-1/PI3K/Akt pathway prevents expression of muscle atrophy, very much important for proper development of muscle tissue [24, 28]. So, skeletal muscle healing is associated with IGF-1.
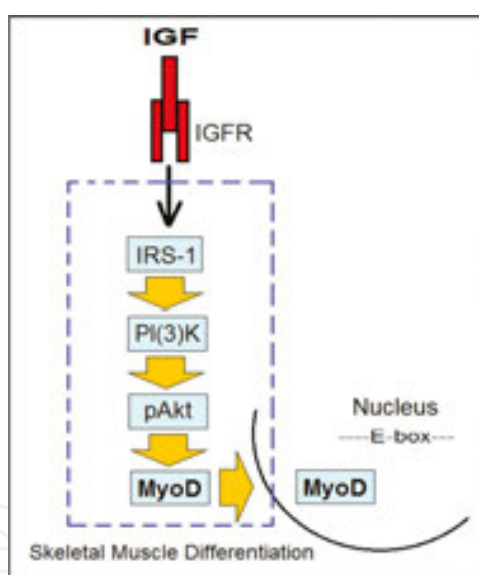

Figure 26. A schematic representation of IGF-1 cell signalling pathway that is involved in skeletal muscle differentiation and maturation.

5.3.2. Protein expression for IGF pathway

To study IGF pathway, expression of IRS-1/PI(3)K/Akt/MyoD proteins is important. Initially, the expression of IRS-1/PI(3)K/Akt/MyoD proteins on GO, GO-PCL and control (tissue culture plate) substrates (**Figure 27**) was analysed. All of these proteins expressed better on GO and GO-PCL, while the expression was highest for GO-PCL. This indicates that the GO-PCL substrate is the most suitable candidate for myoblast differentiation of CB-hMSCs.

To evaluate IGF-1 pathway, Akt is the most important protein that regulates skeletal muscle differentiation and hypertrophy. It was also reported that IGF-1 dependent Akt-phosphoralization increased along with higher rate of myogenic differentiation. Properties of MyoD, responsible for skeletal muscle differentiation, are controlled by Akt and blockage of Akt prevents formation of skeletal muscle transcriptosome [24–26]. The present investigation demonstrates that the investigated pathway proteins expressed better on GO-PCL composite meshes than those on GO sheet or control (tissue culture plate). Up-regulation of such pathway proteins on GO-PCL further emphasize the IGF-1 pathway which is related to skeletal muscle development. Thus, it reveals the importance GO-PCL composite meshes for skeletal muscle tissue engineering applications.
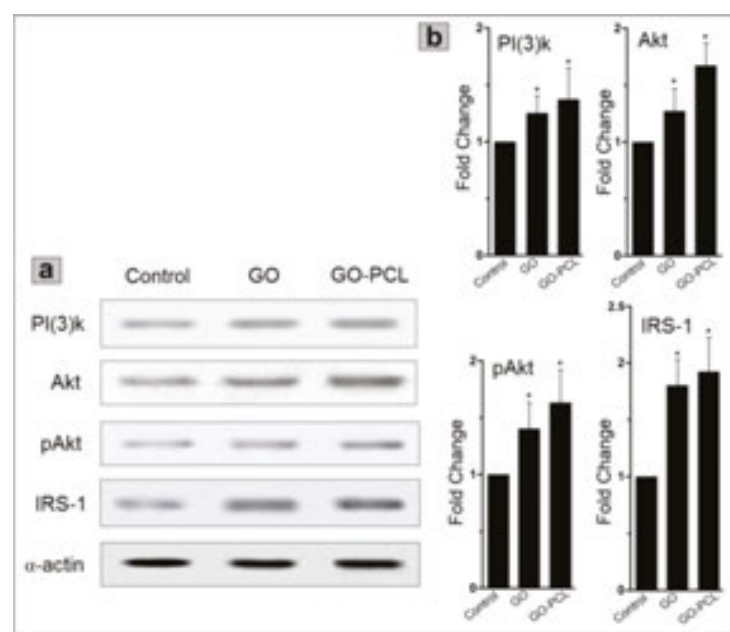

Figure 27. Expression of PI(3)k, Akt, pAkt, IRS-1 (a) and expression of fold change for these corresponding signalling proteins (b) on control (tissue culture plate), GO sheet and GO-PCL meshes. * indicates significant difference ($p < 0.05$).

5.3.3. Effect of Akt inhibition on MyoD expression

As mentioned above, Akt is a major component that regulates IGF-1 pathway. Inhibition of Akt deters IGF-I-stimulated nuclear translocation of Akt and also suppresses the growth of various cells. Akt is a vital component of the cell survival pathway as it functions by resisting apoptosis via improving communication between cells that are damaged [26, 27]. Inhibition of Akt results in much higher rate of apoptosis and a decrease in IGF-1 cell signalling. Inhibition of Akt was done using 10-DEBC hydrochloride, a selective and precise cell permeable Akt phosphorylation inhibitor that shows no activity at PDK1, SGK1 or PI 3-kinase [27, 28]. In the present experiment, the expression of MyoD, a vital myogenic protein that helps in myogenic differentiation has been studied by pre- and post-Akt inhibition. The results showed (**Figure 28**) that after inhibition of Akt, the expression of MyoD intensity decreased rapidly. Akt inhibitor inhibits IGF-I-stimulated nuclear translocation of Akt that results in much reduction

of MyoD protein assessed by Western blotting. This finding indicates the importance of IGF-1/ IRS-1/PI(3)K/Akt/MyoD cell signalling pathway for the system of present investigation.
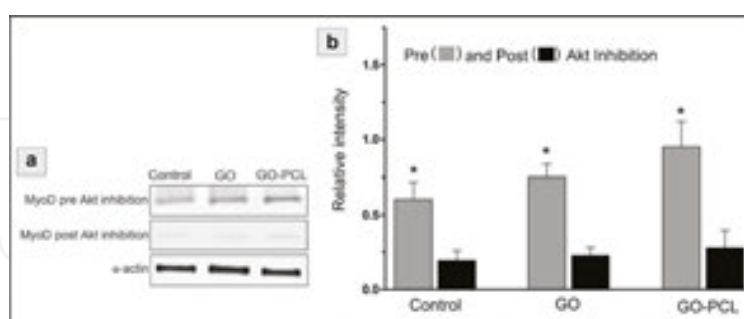
Figure 28. Expression of MyoD (a) and the corresponding relative intensity (b) indicating pre- and post-inhibition of Akt. * indicates significant difference from post Akt inhibition ($p < 0.05$).

The expressions of myogenic proteins on graphene oxide-based substrates (GO sheet and GO-PCL scaffold) have been assessed. It has been demonstrated that myogenic proteins expressed better on the GO-PCL composite meshes than GO sheet and the control (tissue culture plate). This highlighted the superiority of grapheme-based substrates for myoblast differentiation. Favourable physicochemical and biological properties established these scaffolds as potential platforms for myogenic differentiation and maturation for tissue engineering and other biomedical applications. In addition, we have also shown preliminary study of IGF-1 pathway that is important for skeletal muscle differentiation and maturation as well. This pathway proteins (IRS-1/PI(3)K/Akt/MyoD) also expressed better on graphene based substrates, particularly on GO-PCL scaffolds. Moreover, selective inhibition of Akt has reduced the expression level of MyoD, a myogenic protein important for skeletal muscle differentiation.

Hence, it was noticed that lower expression of MyoD along with Akt inhibition indicated the importance of the IGF-1 cell signalling pathway observed from this preliminary investigation. Further elaborate study seems to be more interesting.

6. Conclusion

ElectrospunGOnPs-PCL and GOnPs-PLGA composite scaffolds showed enhanced conductivity and dielectric permittivity due to quantum tunnelling between the graphene oxide nanoflakes. Improved conductivity of the scaffold enhanced biocompatibility of the GOnPs-polymer composite fibrous meshes compared to those of pure polymers like PCL and PLGA. As a consequence, the composite scaffolds showed excellent myoblast differentiation of umbilical cord blood derived mesenchymal stem cells. Increased biocompatibility of GO and GO-polymer composites were attributed to the surface charge and nanoflake structure of graphene oxide. Compared to GOnPs-PLGA, GonPs-PCL composite scaffold meshes exhibited better myoblast differentiation capability which is attributed to the more conducting behaviour of the GOnPs-PCL composite. IGF-1 cell signalling pathway study carried out on the composite

scaffold meshes also showed potentiality for excellent myoblast differentiation and proliferation of cord blood stem cells (CB-hMSCs).Therefore, in demand of cell specific substrates, the use of GO-based polymer composite meshes might be considered as the most potential substrates for the next generation tissue engineering and other biomedical applications. Moreover, it is also worthwhile to mention that cost effective and easily available umbilical cord blood is an important and abundant source of human stem cells for the differentiation of skeletal muscle tissues or other lineages.

Acknowledgements

Author details

Biswadeep Chaudhuri

Address all correspondence to: chaudhuri_biswadeep@rediffmail.com

Department of Biotechnology and Medical Engineering, National Institute of Technology, Rourkela, Odisha, India

References

[1] Novoselov KS. Materials in the flatland. Rev. Mod. Phys. 2011, 83: 837–849.

[2] Agarwal S, Wendorff JH, Greiner A. Use of electrospinning technique for biomedical applications. Polymer. 2008, 49: 5603–5621.

[3] Lee EJ, Lee JH, Shin YC, Hwang DG, Kim JS, Jin OS, Lin L, Hong SW, Han DW. Graphene oxide decorated PLGA/collagen hybrid fibre sheet for application to tissue engineering scaffolds. Biomater. Res. 2014, 18: 18–24.

[4] Choi JS, Lee SJ, Christ GJ, Atala A, Yoo JJ. The influence of electrospun aligned poly(epsilon-caprolactone)/collagen nanofiber meshes on the formation of self-aligned skeletal muscle myotubes. Biomaterials. 2008, 29: 2899–2906.

[5] Chen MC, Sun YC, Chen YH. Electrically conductive nanofibers with highly oriented structures and their potential application in skeletal muscle tissue engineering. Acta Biomaterialia. 2013, 9:5562–5572.

[6] Chaudhuri, Bhadra D, Moroni L, Pramanik K. Myoblast differentiation of human mesenchymal stem cells on graphene oxide and electrospungraphene oxide–polymer composite fibrous meshes: importance of graphene oxide conductivity and dielectric constant on their biocompatibility. Biofabrication. 2015, 7: 1–13. doi: 10.1088/1758-5090/7/1/015009.

[7] Salavagione HJ, G. Martinez G, Gomez MA. Synthesis of poly(vinyl alcohol)/reduced graphite oxide nanocomposites with improved thermal and electrical properties. J. Mater. Chem. 2009, 19: 5027–5032.

[8] Zhao X, Zhang Q, Chen D, Lu P. Enhanced mechanical properties of graphene-based poly(vinyl alcohol) composites. Macromolecules. 2010, 43: 2357–2363.

[9] Rivers TJ, Hudson TW, Schmidt EC. Synthesis of a novel, biodegradable electrically conducting polymer for biomedical applications. Adv. Funct. Mater. 2002, 12: 33–37.

[10] Ryu S, Kim BS. Culture of neural cells and stem cells on graphene. Tissue Eng. Regener. Med. 2013, 10: 39–46.

[11] Sun X, Liu Z, Welsher K, Robinson JT, Goodwin A, Zaric S, Dai H. Nano-graphene oxide for cellular imaging and drug delivery. Nano Res. Lett. 2008, 1: 203–312.

[12] Liu Z, Robinson JT, Sun X, Dal H, PEGylated nanographene oxide for delivery of water insoluble cancer drug. J. Am. Chem. Soc. 2008, 130:10876–10877.

[13] Nayak, AH, Makam VS, Khaw C, Bae S, Xu X, Ee PL, Ahn JH, Hong BH, Pastorin G, Özyilmaz B. Graphene for controlled and accelerated osteogenic differentiation of human mesenchymal stem cells. ACS Nano. 2011, 5: 4670–4678.

[14] Ku SH, Park CB. Myoblast differentiation on graphene oxide. Biomaterials. 2013, 34:2017–2023.

[15] Wang K, Ruan J, Song H, Zhang J, Wo Y, Guo S, Cui D. Biocompatibility of graphene oxide. Nanoscale Res. Lett. 2011, 6: 1–8 .doi: 10.1007/s11671-010-9751-6.

[16] Kim H, Abdala AA, Macosko CW. Graphene/polymer nanocomposite. Macromolecules. 2010, 43: 6515–6530.

[17] Yi JS, Park JS, Ham YM, Nguyen N, Lee NR, Hong J, Kim BW, Lee H, and Lee CS. MG53-induced IRS-1 ubiquitination negatively regulates skeletal myogenesis and insulin signaling. *Nature Communi.* 4: 2354, 2013.

[18] Du XS, Xiao M, Meng YZ, Hay AS. Direct synthesis of poly(acrylenedisulfide)/carbon nanosheet composites via the oxidation with graphite oxide. Carbon. 2005, 43:195–213.

[19] Chaudhuri, BD, Mondal B, Pramanik. Biocompatibility of electrospungraphene oxide poly caprolactone fibrous scaffolds with human cord blood derived mesenchymal stem cells derive skeletal myoblasts. Mater.Lett. 2014, 126:109–112.

[20] Chaudhuri B. Ph.D. Thesis entitled "Development of novel scaffold for skeletal muscle tissue engineering applications", National Institute of Technology, Rourkela, Odishan, India, 2016.

[21] Berridge MJ. Cell Signaling Biology (Signalling Defects and Disease), Module 12. 2014, doi:10.1042/csb0001012, 2014.

[22] Harada H, Andersen JS, Mann M, Terada N, Korsmeyer SJ. p70S6 kinase signals cell survival as well as growth, inactivating the pro-apoptotic molecule BAD. Proc. Natl. Acad. Sci. U.S.A. 2001,98: 9666–9670.

[23] Akhavan O, Ghaderi E, Shahsavar M. 2013 Graphenenanogrids for selective and fast osteogenic differentiation of human mesenchymal stem cells. Carbon.2013, 59: 200–2211.

[24] Zhang LM, Xia JG, Zhao QH, Liu LW, Zhang ZJ. Functional graphene oxide as a nanocarrier for controlling loading and targeted delivery of mixed anticancer drugs. Small. 2010, 6: 537–544.

[25] Chen GY, Pang DW, Hwang SM, Tuan HY, Hu YC.A graphene-based platform for induced pluripotent stem cells culture and differentiation. Biomaterials. 2012, 33: 418–427.

[26] Yi JS, Park JS, Ham YM, Nguyen N, Lee NR, Hong J, Kim BW, Lee H, and Lee CS. MG53-induced IRS-1 ubiquitination negatively regulates skeletal myogenesis and insulin signaling. Nature *Communi*. 4: 2354, 2013.

[27] Lee CS, Yi JS, Jung SY, Kim BW, Lee NR, Choo HJ, Jang SY, Han J, Chi SG, Park M, Lee JH, Ko YG. TRIM72 negatively regulates myogenesis via targeting insulin receptor substrate-1. Cell Death Differ.(Nature Publishing Group). 2010, 17: 1254–1265.

[28] Stitt TN, Drujan D, Clarke BA, Panaro F, Timofeyva Y, Kline WO, Gonzalez M, Yancopoulos GD, and Glass DJ. The IGF-1/PI3K/Akt pathway prevents expression of muscle atrophy-induced ubiquitin ligases by inhibiting FOXO transcription factors. Mol. Cell. 14(3):395–403. 2004.